JOURNAL of
MATERIALS and MECHATRONICS:A

e-ISSN 2717-8811
JournalMM, 2021, 2(2), 60-71

Araştırma Makalesi / Research Article

Front Suspension System Design of the Lightweight Solar-Powered Vehicle

Talha Batuhan KORKUT[1], Zeynep PASİNLİ[2], Aytaç GÖREN[3,4]*

[1] Dokuz Eylul University, The Graduate School of Natural and Applied Sciences, Mechatronics Engineering, Izmir, Turkey, ORCID ID: https://orcid.org/0000-0002-1166-6700, tbatuhankorkut@outlook.com
[2] Dokuz Eylul University, Department of Mechanical Engineering, Automatic Control and Robotic Labs, Izmir, Turkey, ORCID ID: https://orcid.org/0000-0002-6283-6933, zeyneppasinli@gmail.com
[3] Laboratory of Innovative Technologies, Picardie Jules Verne University, Amiens, France, ORCID ID: https://orcid.org/0000-0002-7954-1816, aytac.goren@u-picardie.fr
[4] Dokuz Eylul University, The Graduate School of Natural and Applied Sciences, Mechatronics Engineering, Izmir, Turkey, ORCID ID: https://orcid.org/0000-0002-7954-1816, aytac.goren@deu.edu.tr

Geliş/ Received: 05.03.2021; **Kabul / Accepted:** 15.04.2021

ABSTRACT: The main principle encouraging by solar cars is the potentiality to produce energy from the sun with an attitude that respects the environment. Increasing interest in solar-powered vehicles arise as a topic of study mainly developed by academic institutions, students, engineers, researchers, and also solar car teams all around the world with the aim of promoting sustainable mobility, gives us the opportunity that enhances the make the more efficient solar car with include proper optimization on its mechanics like the suspension system, steering system, vehicle's dynamics, etc. In this study, the finite element analysis of the front suspension system of the solar-powered vehicle was carried out. The regions to be optimized on the relevant suspension system parts were carried out by a topology optimization study. After that, parts and geometries of the new suspension system were designed. The main object of this study is mass optimization of the new suspension system.

Keywords: Solar-Powered vehicle, Suspension system, Knuckle arm, Double wishbone.

*Sorumlu yazar / Corresponding author: aytac.goren@deu.edu.tr

Bu makaleye atıf yapmak için /To cite this article

Korkut, T.B., Pasinli, Z., Gören, A. (2021). Front Suspension System Design of the Lightweight Solar-Powered Vehicle. Journal of Materials and Mechatronics: A (JournalMM), 2(2), 60-71.

Güneş Enerjili Hafif Aracın Ön Süspansiyon Sistemi Tasarımı

ÖZET: Güneş arabalarının özendirici temel ilkesi, çevreye saygılı bir tavırla güneşten enerji üretme potansiyelidir. Güneş enerjisiyle çalışan araçlara artan ilgi, temel olarak akademik kurumlar, öğrenciler, mühendisler, araştırmacılar ve ayrıca dünyanın dört bir yanındaki güneş enerjili araba ekipleri tarafından sürdürülebilir hareketliliği teşvik etmek amacıyla geliştirilen bir çalışma konusu olarak ortaya çıkmaktadır. Daha verimli araç, daha verimli süspansiyon sistemi, direksiyon sistemi, aracın dinamikleri gibi mekaniği üzerinde uygun optimizasyon çalışmalarını içermesi, alandaki çalışmalara yön vermesi anlamında önem arz etmektedir. Bu çalışmada, güneş enerjili aracın ön süspansiyon sisteminin sonlu eleman analizi yapılmıştır. İlgili askı sistemi parçaları üzerinde optimize edilecek bölgeler, bir topoloji optimizasyon çalışması ile gerçekleştirilmiştir. Devamında, yeni süspansiyon sisteminin parçaları ve geometrileri tasarlanmıştır. Bu çalışmanın ana amacı, yeni süspansiyon sisteminin kütle optimizasyonudur.

Anahtar Kelimeler: Güneş arabaları, Süspansiyon sistemi, Yön verme mafsal kolu, Çift salıncak.

1. INTRODUCTION

Energy is indispensable to modern society, unfortunately, most primary sources are unsustainable. Nonrenewable resources are associated with a multitude of environmental impacts, including global climate change, acid rain, freshwater consumption, hazardous air pollution, and radioactive waste. Nevertheless, renewable energy has the potential to meet demand with a much smaller environmental footprint and can help to alleviate other pressing problems, such as energy security, by contributing to a distributed and diversified energy infrastructure. However, wind and solar as major renewable sources are the fastest growing renewable sources, but their contribution is much smaller of the total energy usage of the world rankings (Anonymous, 2020).

From the consumption as well as the production point of view, renewable energy sources are finding their value in the automotive industry. While the automotive companies are willing to develop environmentally-friendly vehicles and introduce sustainable production processes, there is further potential space for renewable energy sources. To illustrate, innovative automotive companies in Germany are investing in sustainable energy projects as part of their company strategy aligning with "Energiewende" politics (Pechancová, 2017).

Renewable energy also plays a role in boutique race teams of academic origin such as solar car teams in the worldwide. In fact, we are writing this academic study based on Solaris 11 solar-powered vehicle, one of the boutique solar racing teams we mentioned. As part of the solar car team, we aim at development and innovation in our new vehicles every year. Therefore, this study brings along suspension optimization, which is a vital parameter in vehicle design.

The suspension system of a car performing a vital role on the vehicle's stability. Cars must be overcome the surrounding resistance's inertia with the effective design of suspension system design that could dissipate through ground vibrations and absorbs the detrimental influence of road conditions (Harris, 2020; Camargo et al., 2017) The idea of structural optimization of suspension system gather around two important considerations: stiffness and durability. Hereat the design parameters evaluate for making the suspension lighter, compact, and ensuring it always stays in contact with road during several maneuvers (Camargo et al., 2017). Thus, the suspension system design does not belong to only meet the basic requirements of the vehicle like absorption and safety

but also augment the performance of the solar car where the energy management is a particularly important issue.

Felipe Vannucchi de Camargo et al. have investigated the suspension system of a solar-powered vehicle at their work. They were enhanced three different shapes made out of carbon fiber reinforced plastic was analyzed and compared through static and modal finite element analysis (Camargo et al., 2017).

Burdick et al. have main purpose to optimize their 2016 suspension system which is 15.83 kg more than their 2020 solar car's suspension weighed. Their design consists of a leading double control arm suspension in the front and a trailing arm suspension in the rear. A bell crank shock is used for both systems. All components were mounted to a three-layer M10 carbon fiber chassis board which was selected based on material testing (Burdick et al., 2019)

Odabasi et al. are in their study a preliminary comparison was presented among longitudinal arms with leaf springs, MacPherson and double wishbone, aimed at pointing out the most appropriate design for the solar-powered vehicle hereby considered, considering its its specific demands for low-weight and efficient structures (Odabasi et al., 2018)

2. MATERIALS AND METHODS

2.1 Materials

The suspension system isolates the vehicle and occupants from the vibration of the road surface. When the solar-powered vehicle hits bumps, the suspension system provides handling and steering of the solar car. Before designing the suspension system, the balance of the solar-powered vehicle should be calculated and specified the spring and damper rates for the front and rear wheels. For these calculations' wheelbase, the weight of the car, and the moment of inertia of the solar car must be known. The weight of Solaris 11 is about 2750 N and the wheelbase is typically 2.0 m. Solaris 11 is a solar car that is three-wheeled with two wheels in front and a single rear wheel. All of the tires must be loaded approximately equal weight for stability.

The main weights of the solar-car were assumed to be 785 N for the driver, 200 N for the battery, 150 N for the brushless DC motor, 150 N for the solar array, and 540 N for the monocoque body-chassis. The center of gravity for the 540 N monocoque chassis is assumed to be at the center of the body. The driver and battery weights have been moved to obtain the required 51.5% of the weight on the front wheels. The polar moment of inertia can be calculated after specifying the center of gravity.

A double-wishbone suspension has been chosen to use for the solar-powered vehicle. Because double-wishbone suspension provides the best control of the suspension geometry and it is lighter than the McPherson suspension type. Before enhancing the suspension design, the wheelbase and wheel track must be determined. The wheel track and wheelbase have been determined as 0.8 m and 2.0 m. The following items have been taken into consideration during the design of suspension geometry.

•Lower wishbones in the suspension are longer than the upper wishbones. Longer lower wishbones reduce the scrub and bump steer. These design criteria can be possible with the narrow chassis structure. Also, a wider wheel track provides longer lower wishbones.

•The lower wishbones conduct higher loads to the chassis than the upper wishbones. Therefore, points where the wishbones hook onto the chassis, must be stiff.

•Another critical consideration is the distance between the lower and upper wishbones. If the distance can be increased, death wobble can be reduced. Another point of view, the larger distance can be contributed to reducing loads on the upper wishbone, and scrub, bump steer can be minimized.

After the calculated wishbones length, the next step is the defining kingpin axis. Angling the kingpin through the center of the tire patch provides the braking loads to are having a zero moment around the kingpin axis. This condition eliminates the brake steer.

Table 1. Mechanical properties of aluminum 7074 T6 and AlSi7Mg alloy

Material Properties	Magnitude with Units of Aluminum 7075 T6	Magnitude with Units of AlSi7Mg
Density [kg/m^3]	2880	2660
Tensile Strength [MPa]	510-538	220
Poisson's Ratio	0.33	0.33
Young Modulus [MPa]	71.7	74
Elongation at Break [%]	11	2.5

2.2 Force Calculation

Before the finite element analysis and part designs, the forces acting on the vehicle should be calculated. As shown in figure 1, three types of forces act on the solar-powered vehicle. These are braking, axial, and radial forces. The radial force is the force perpendicular to the ground acting on the wheel and it is a force that occurs depending on the mass of the relevant land vehicle. Axial force, on the other hand, is a force that depends on mass, speed, and radius of turn.

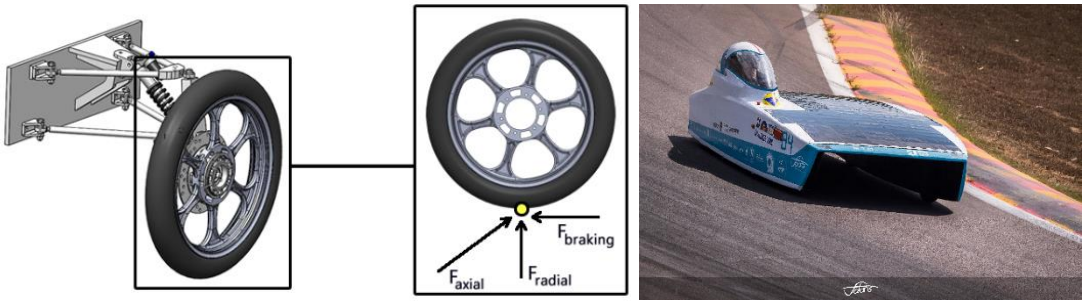

Figure 1. Forces acting on the solar-powered vehicle

The mass of the Solaris 11 vehicle was assumed to be 280 kg. The safety factor was accepted as 2 in the radial force calculation. Because it is assumed that the entire mass is formed on 2 wheels while the vehicle turns around the bend. The radial force calculation has shown in equation 1.

$$m\ x\ g\ x\ SF = 82.6\ x\ 9.81\ x\ 2 = 1620.612\ N \quad (1)$$

As a result of examining the road data of Solaris Solar Car Team in axial force calculation, it was determined that the turning radius of the most critical scenario was recorded while turning with a speed of 16.67 m/s at a 38.9 m bend. The axial force calculation has shown in equation 2.

$$\frac{mv^2}{r} xSF = \frac{82.6\ x\ 16.67^2}{33.875} x1.5 = 1016.397\ N \quad (2)$$

In this solar-powered vehicle, it has been decided to use hydraulic disc brakes at the front and rear. In this study, the main focus on the front axle. The solar-powered vehicle designed for the participating Bridgestone World Solar Challenge. In scrutineering, all solar-powered vehicles test for

braking capability. When the velocity is 60 km/h, all vehicles have to stop in 30 meters. For this reason, the first step is calculating the kinetic energy of the solar car in the first braking force.

$$KE = 0.5\ x\ m\ x\ V^2 = 38904.45\ J \tag{3}$$

Stopping distance calculation as,

$$s = 0.1\ x\ v + 0.0060\ x\ v^2 = 27.6\ m \tag{4}$$

Average braking force calculation as,

$$F_{avg} = \frac{mv^2}{2s} = 1409.581 \tag{5}$$

Deceleration,

$$D_x = 0.5g \tag{6}$$

Stopping time calculation as,

$$V = U - D_x\ x\ t => 3.4\ seconds \tag{7}$$

Dynamic weight transfer calculation as,

$$W_D = \left(\frac{h}{L}\right) * \left(\frac{W}{g}\right) * D_x = 586.1671\ N \tag{8}$$

The radial load on the front axle calculated 1620.612 N and the rear axle is 1126.188 N. In dynamic condition vertical load on the front and rear axles,

$$\begin{gathered} Front\ Axle = 1620.612 + W_D = 2206.779\ N \\ Rear\ Axle = 1126.188 - W_D = 540.0209\ N \end{gathered} \tag{9}$$

Percentage load transfer while braking,

$$\begin{gathered} Front\ Axle\ Percent = 0.8034 \\ Rear\ Axle\ Percent = 0.1966 \end{gathered} \tag{10}$$

Required braking force at the front and rear axles,

$$\begin{gathered} F_{front,required} = 1132.005\ N \\ F_{rear,required} = 277.0129\ N \end{gathered} \tag{11}$$

Braking torque required for a single front wheel,

$$T_F = \frac{Brake\ Force}{2} * \mu * Effective\ Radius\ of\ Wheel = 47.385\ Nm \tag{12}$$

Braking torque required for a single rear wheel,

$$T_F = \frac{Brake\ Force}{2} * \mu * Effective\ Radius\ of\ Wheel = 23.192\ Nm \quad (13)$$

Table 2. Force calculation study of Solaris 11 solar-powered vehicle

#	Type	Force [N]
1	Radial	1620.612
2	Axial	1016.397
3	Brake	566.0025

2.3 Spring Rate Calculation

One of the main purposes of suspension is to generate as much grip as possible from the tires in order to keep the tires in contact with the road, because it is the friction between the tires and the road that affects a vehicle's ability to steer, brake and accelerate.

Finding the ideal spring rate of the purpose-built solar race car plays a major role in the choice of suspension spring. Primary objective of the calculating ideal spring rates for a car is that calculations are based on ideal wheel loadings of the car. However, the ideal wheel loadings require ideal spring rates to calculate from. Due to this reason, a typical design problem is occurred. In order to overcome this issue, we need to calculate our ideal spring rate with appropriate assumptions to fine tune. When we calculate the ideal spring rate of the solar car, we could choose the appropriate suspension spring (coil spring, leaf spring etc.) from the industry.

- If the weight distribution of the solar-powered vehicle is unequal between the front and rear axle, kfront/Wfront should be about 30% less than krear/Wrear.
- The bounce and pitch frequencies should be close together, and the bounce frequency should not be more than 1.2 times the pitch frequency. A higher ratio results in interference kicks that degrade the performance of the suspension.
- For passenger cars, the bounce and pitch frequencies should be about 1.3 Hz or less to give a nice smooth ride. Solar cars can sacrifice a smooth ride for energy efficiency, as long as it does not get into the range of causing the driver motion sickness or dizziness.

Front ride rate calculation as,

$$K_R = (\Delta W x 9.81)/X \text{ [N/mm]}$$
$$\Delta W = Front\ outside\ wheel\ change\ [kg] \quad (14)$$
$$X = Front\ bump\ allowance\ [m]$$

Front ride wheel rate calculation as,

$$K_W = \frac{(K_R + K_T)}{(K_T - K_R)}\ [N/mm]$$
$$K_R = Ride\ rate\ [N/mm] \quad (15)$$
$$K_T = Tire\ vertical\ rate\ [N/mm]$$

Installation ratio calculation as,

$$IR_F = \text{Damper Displacement / Wheel Displacement} \quad (16)$$

Front spring rate calculation as,

$$K_{SF} = K_{WF}/(IR_F)^2 \ [N/mm]$$
$$K_{WF} = Front\ ride\ wheel\ rate\ [N/mm] \quad (17)$$

2.4 Previous and New Suspension Setup

When the solar-powered vehicle crossed the bump, the first contact of the reaction forces happens on the tire and rim. These forces are moved into the suspension arms and are then moved to the actual suspension. Old and new suspension parts were examined. There are many physical differences that are shown between them. Both suspensions setup can divide into 3 main parts. There are knuckle arm, upper and lower wishbones. Specifically, the weights of the old knuckle arm design are 1076.5 grams, the upper wishbone is 598.8 grams and the lower wishbone is 697.18 grams. Besides that, for the new suspension parts, the new knuckle arm design is 489 grams, the upper wishbone is 74.52 grams, and the lower wishbone is 244.63 grams. In conclusion, the weight difference between the two-suspension setup is 1564.33 grams.

There are some physical differences between old and new suspension systems. For instance, the heights of roll centers of front and rear are 0 and 326.05 mm for the old suspension system. The vertical distance between the center of gravity and the roll axis is 25.81 mm. For the new suspension system, the heights of roll centers of the front and rear are 76 and 316 mm. The vertical distance between the center of gravity and the roll axis is 5 mm. Consequently, the calculated amount of torque acting upon the chassis during cornering different for each suspension system. The scenario is a 33 m turning radius and the velocity is 16.67 m/s. The torque acting upon the chassis is 59.28 Nm on the old suspension system and 11.48 Nm on the new suspension system.

The new suspension system has designed for the new solar-powered vehicle. The track width of the old suspension system is 1500 mm, and 800 mm for the new suspension system. The steering and handling conditions are harder for the lower trackwidth. But more efficient aerodynamic bodies have lower track width. Each suspension setups have a positive scrub radius. A positive radius allows the wheel to roll over on lock making parking situations easier. Having a small scrub radius is beneficial as it allows the wheel to react less to braking inputs due to the smaller moment arm and increases steering stability under braking conditions. As shown in Table 3, all physical details of both suspension setups indicated. A hybrid system includes a polymer composite leaf spring and shock absorber at the front suspension at the new suspension setup.

Table 3. Formal engineering specification table of the previous and new suspension set-up

#	Parameters	Value [Previous]	Value [New]
1	Weight	280 kg	280 kg
2	Natural Frequency	2.5 Hz	2.17 Hz
3	Speed	75 km/h	75 km/h
4	Tire Scrub	2.82 mm	5 mm
5	Toe Angle	0 degree	0.5 degrees
6	Track Width	1500 mm	800 mm
7	Wheelbase	2200 mm	2200 mm
8	Height of roll center of front	0 mm	76 mm
9	Height of roll center of rear	326.05 mm	316 mm
10	Height of C.G.	150 mm	196.8 mm
11	The vertical distance between C.G. and roll axis	25.81 mm	5 mm
12	W_R:W_F	0.6949	0.6949
13	Ideal front spring rate	50 N/mm	72.64 N/mm

3. RESULTS AND DISCUSSION

3.1 Previous Suspension System

After the finite element analysis of the old suspension system, the topology optimization study of the old suspension system was carried out. The topology optimization study was made realize on the knuckle arm, a-arms, and brackets of the suspension system. According to the analysis results, the maximum stress distribution in the lower wishbone connection area was observed. The maximum strength in this region was observed around 80 MPa. The stresses seen in the upper wishbone connection area are around 45-50 MPa. The stress difference seen between the two connection areas is 50%. The maximum stress value observed in the lower wishbone parts is 161.55 MPa, and the maximum stress value observed in the upper wishbone parts is 123.65 MPa. In Figure 5, the safety factor studies of all suspension parts were observed. All suspension parts are safe in line with the material properties used. For this reason, the mass reduction has been performed in all parts.

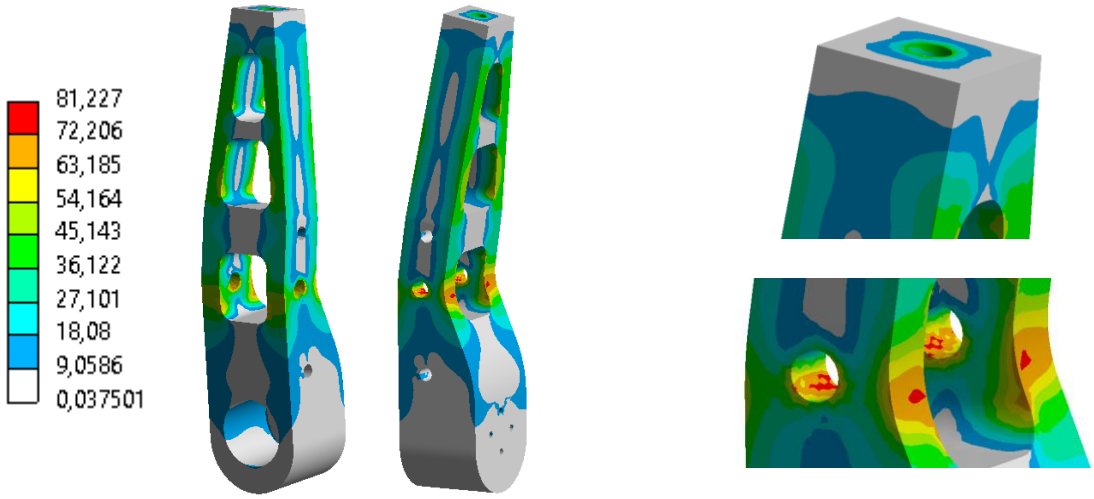

Figure 2. Equivalent stress distribution on old design of knuckle arm [MPa]

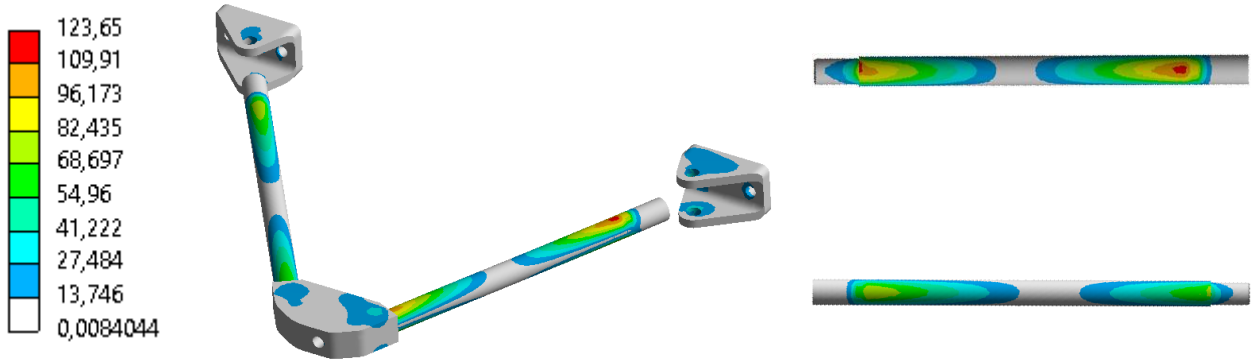

Figure 3. Equivalent stress distribution on old design of upper wishbones [MPa]

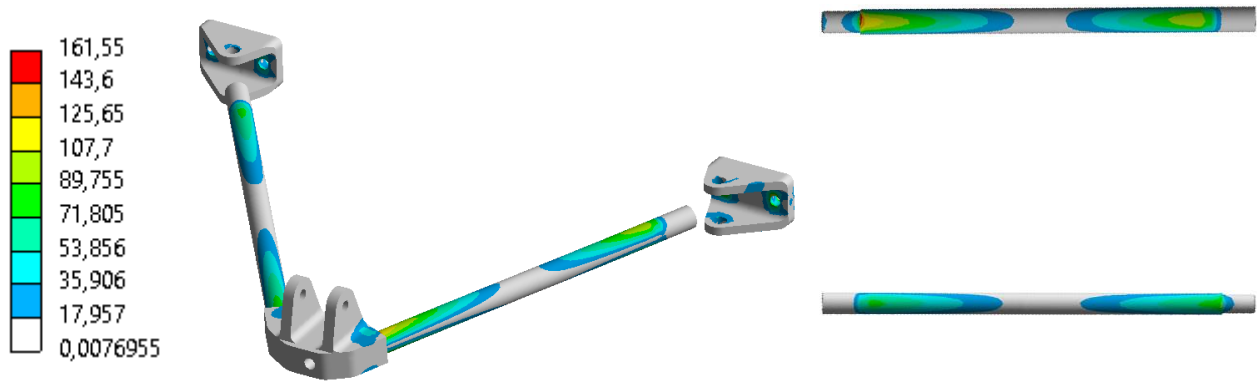

Figure 4. Equivalent stress distribution on old design of lower wishbones [MPa]

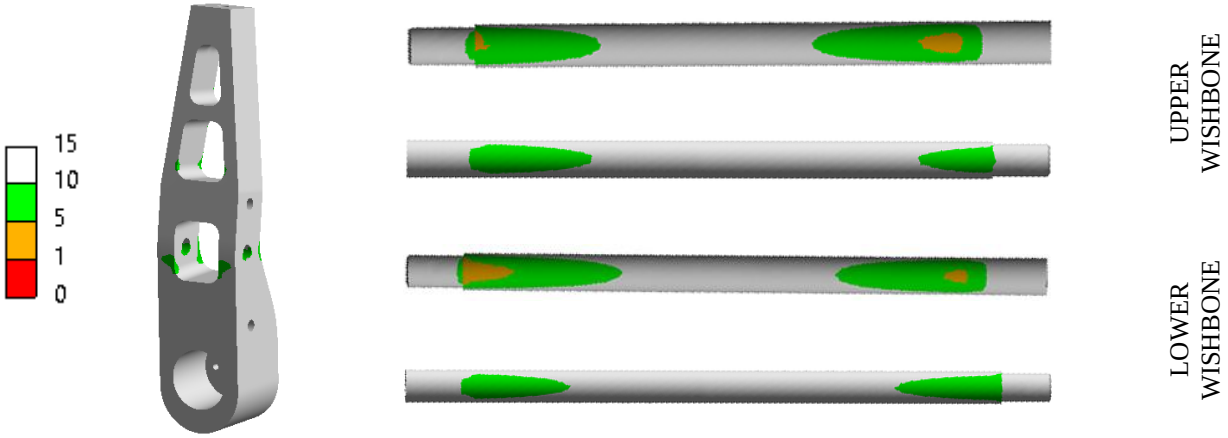

Figure 5. Safety factor study of the old suspension system

3.2 New Suspension System

At the end of the new suspension system study, results showed that the maximum equivalent stress occurred on the upper wishbones. The average occurred stress on the knuckle arm design is 8.27 MPa and the maximum stress is 76.66 MPa. The stresses seen in the upper wishbone connection area are around 50-55 MPa and on the lower wishbone are 65-70 MPa. The maximum stress value observed in the lower wishbone parts is 23.47 MPa, and the maximum stress value observed in the upper wishbone parts is 48.62 MPa. Reduction of the occurred stress and mass amounts are shown in table 4. Safety factor studies were shown in Figure 9 and observed. All suspension parts are safe in line with the material properties used.

Table 4. Mass reduction studies in the new suspension systems

Part Name	Mass [gram]		Difference [%]
	Old	New	
Knuckle Arm	1076.5	489	%54.58
Upper Wishbone	598.8	74.52	%87.56
Lower Wishbone	697.18	244.63	%64.91
Total	2372.48	808.15	%65.94

Table 5. Maximum equivalent stress occurred on suspension parts

Part Name	Equivalent Stress [MPa]		Difference [%]
	Old	New	
Knuckle Arm	81.227	76.662	%5.62
Upper Wishbone	123.65	48.616	%60.68
Lower Wishbone	161.55	23.466	%85.47

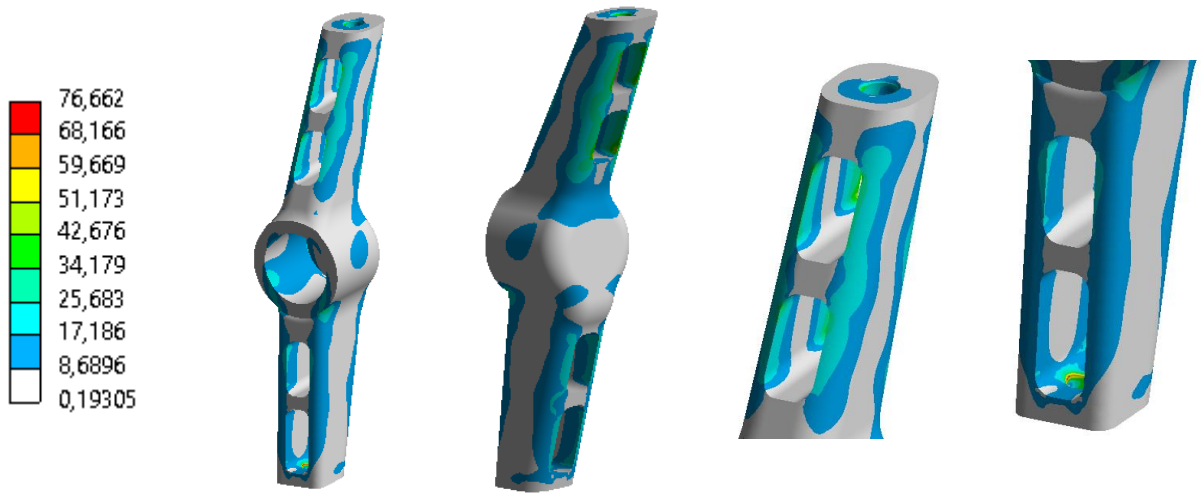

Figure 6. Equivalent stress distribution on new design of knuckle arm [MPa]

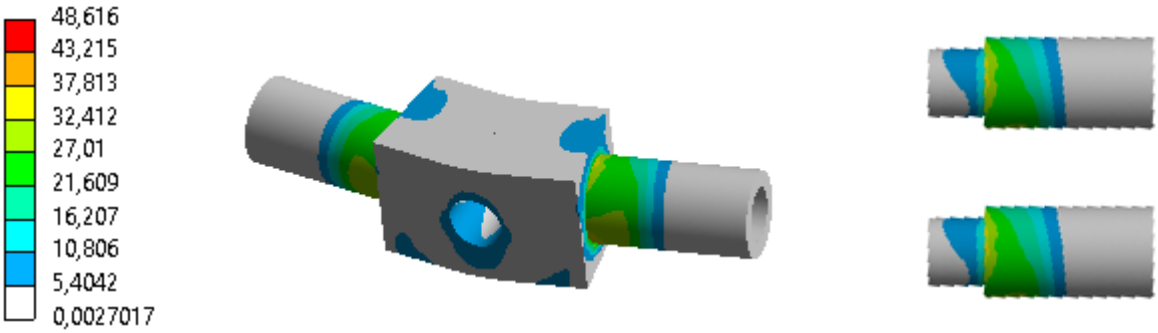

Figure 7. Equivalent stress distribution on new design of upper wishbones [MPa]

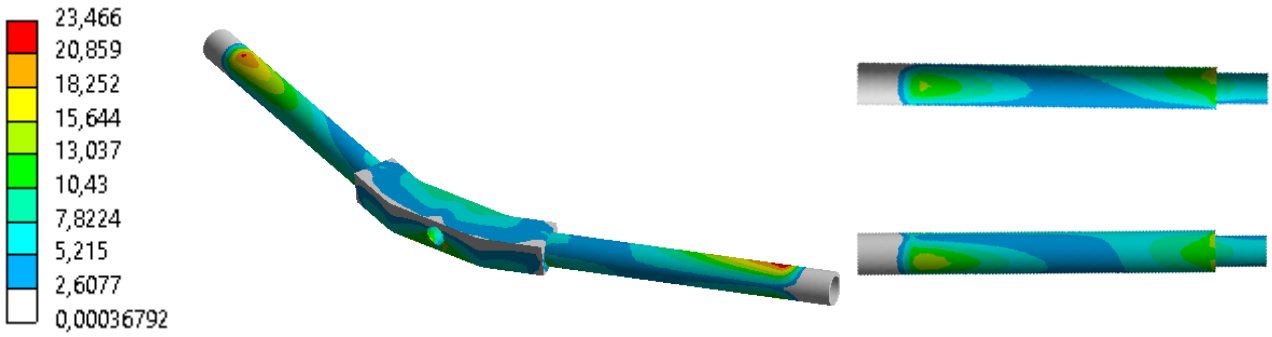

Figure 8. Equivalent stress distribution on new design of lower wishbones [MPa]

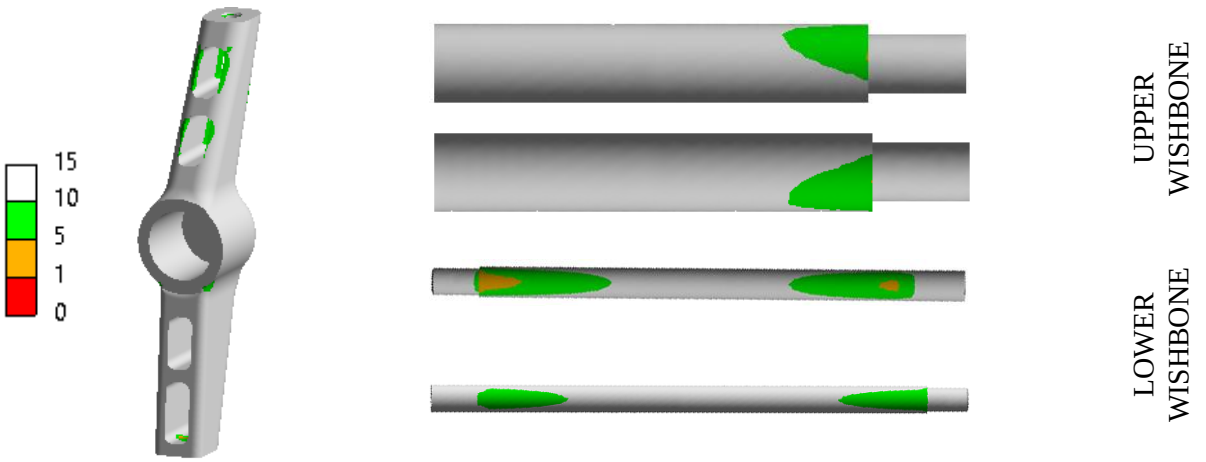

Figure 9. Safety factor study of the new suspension system

Another important issue in the design of the new suspension system is the kinetic analysis of the relevant wishbone mechanism. Because the upper and lower wishbones may not design to be parallel to each other and this mechanism can be locked when the vehicle is on road. For this reason, the spring and shock absorber may not work properly and this may happen the bump steer on the vehicle. Figure 10 shows that the unstable angles of the lower and upper wishbones of the new suspension system with the ground. Upper and lower wishbones work at close angles with each other and they conduct the reaction force to the shock absorber and spring as accurately.

Figure 10. Motion study of wishbones of the new suspension system

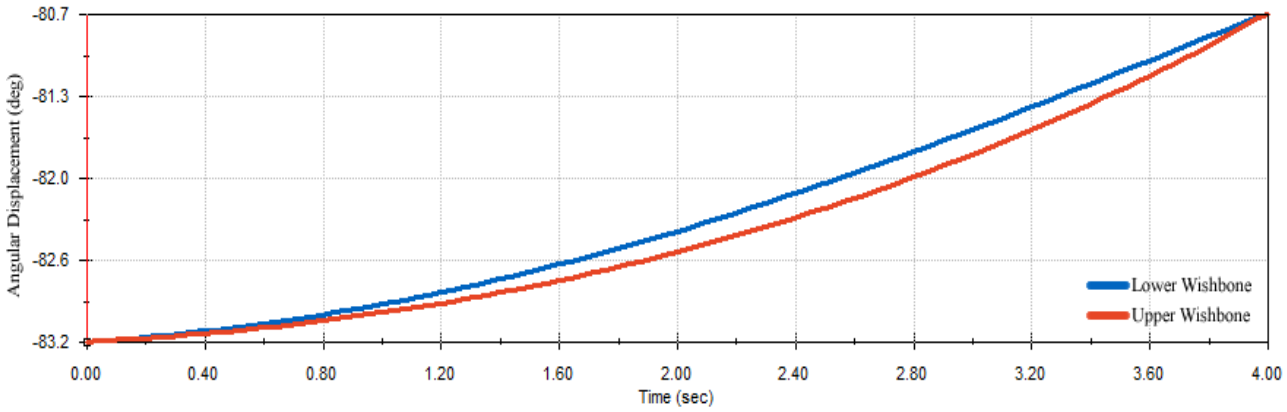

4. CONCLUSION

In this study, the static analysis of the aluminum alloy suspension system parts designed for a solar-powered vehicle was carried out and strengthening and weight reduction studies were conducted. It has been observed that weight and mechanical properties can be improved by different design approaches and material selections. The conclusions are given below:

- According to finite element analysis (FEA) results, it was concluded that a weight reduction may be applied at regions where the low equivalent stresses are observed. The final design has a 65.94% (1.564 kg) weight reduction compared to the initial design (2.372 kg).
- The maximum equivalent stress of the new suspension system parts also reduced by 5.62% on the knuckle arm design, by 6.06% on the upper wishbone, and by 80.23% on the lower wishbone.

5. ACKNOWLEDGEMENTS

The authors would like to thank S11 Solaris Team members for their help in the implementation of Finite Element Analysis and performing tests.

6. CONFLICT OF INTEREST

Author approve that to the best of their knowledge, there is not any conflict of interest or common interest with an institution/organization or a person that may affect the review process of the paper.

7. AUTHOR CONTRIBUTION

Taha Batuhan KORKUT contributed management of the conceptual and design processes of the study, data analysis and interpretation, creation of the draft paper, critical analysis of the intellectual content. Zeynep PASİNLİ, contributed to the determination and management of the conceptual and design processes of the study, data collection and preparation of the manuscript. Aytaç GÖREN contributed final approval and full responsibility.

8. REFERENCES

Arsie I., Rizzo G., Sorrentino M., Optimal design and synamic simulation of a hybrid solar vehicle. SAE Technical Paper 2006-01-2997, 2006.

Bastow D., Howard G., Car suspension and handling, Society of Automotive Engineers, Third Edition Warrendale, PA, 1993.

Burdick I., Haynes C., Patzer N., Lightweight racing suspension project, Senior Design Project, Western Michigan University, 2019.

Camargo F. V., Fragassa C., Pavlovic A., Martignani M., Analysis of the suspension design evolution in solar cars, FME Transactions 45(3), 394-404, 2017.

Center for Sustainable Systems, University of Michigan, U.S. Renewable Energy Factsheet, Pub. No. CSS03-12, 2020.

Dhir N. S., Design and optimization of suspension geometry of a solar electric passenger vehicle, International Research Journal of Engineering and Technology 5(11), 207-214, 2018.

George B., Benny A. T., John A., Jose A., Francis D., Design and fabrication of steering and bracking system for all terrain vehicle, International Journal of Scientific and Engineering Reaserch 7(3), 7-18, 2016.

Gillespie T. D, Fundamentals of Vehicle Dynamics, Society of Automotive Engineers, Warrendale, PA, 1992.

Harris W., 2020. How car suspensions work, https://auto.howstuffworks.com/car-suspension.htm (Date of Access: 06.02 2020).

Kawade G. H., Pharande R. D., Patil S. B., Design of steering and braking system for a solar car, International Journal for Research in Engineering Application & Management 4(10), 333-340, 2019.

Korkut T. B., Armakan E., Özaydin O., Gören A., Design and comparative strength analysis of wheel rims of a lightweight electric vehicle using Al6063 T6 and Al5083 aluminium alloys, Journal of Achievements of Materials and Manufacturing Engineering 2(99), 57-63, 2020.

Milliken W. F., Milliken D. L., Race car vehicle dynamics, Society of Automotive Engineers, Warrendale, PA, 1995.

Odabaşı V., Maglio S., Martini A., Sorrentino S., Static stress analysis of suspension systems for a solar-powered car, FME Transactions 47(1), 70-75, 2019.

Pechancová V., Renewable energy potential in the automotive sector: Czech regional case study, Journal of Security and Sustainability Issues 6(4), 537-545, 2017.

Roche D. M., Schinckel A. E. T., Storey J. W. V., Humphris C. P., Guelden M. R., Speed of light: The 1996 World Solar Challenge, Photovoltaics Special Research Center, University of New South Wales, Sydney, Australia, 1997.

Storey J. W. V, Schinckel A. E. T., Kyle C. R., Solar Racing Cars, Australian Government Publishing Service, Canberra, Australia, 1994.